
Oral presentation | Industrial applications

Industrial applications-III

Tue. Jul 16, 2024 2:00 PM - 4:00 PM Room B

[5-B-04] A Hybrid Finite Volume/Element Method for Studying Liquid Argon Time Projection Chamber Detectors

*Shuang Zhang Tu¹, Chao Jiang¹, Qing Jane Pang¹ (1. Jackson State University)

Keywords: Incompressible flow, Space charge, LArTPC Detector, Hybrid finite volume/element method

A Hybrid Finite Volume/Finite Element Solver for Investigating the Space Charge Effect on the Electric Field in Liquid Argon Time Projection Chambers Detectors

Shuang Tu, Chao Jiang and Q. Pang
Fermilab collaborators: Tom Junk and Tingjun Yang

Jackson State University and Fermilab

ICCFD12, July 2024, Kobe, Japan

Outline

- 1 Background
- 2 Governing Equations
- 3 Numerical Methodology
- 4 Solver Parallelization
- 5 Test Cases
- 6 Summary and Future Work

Outline

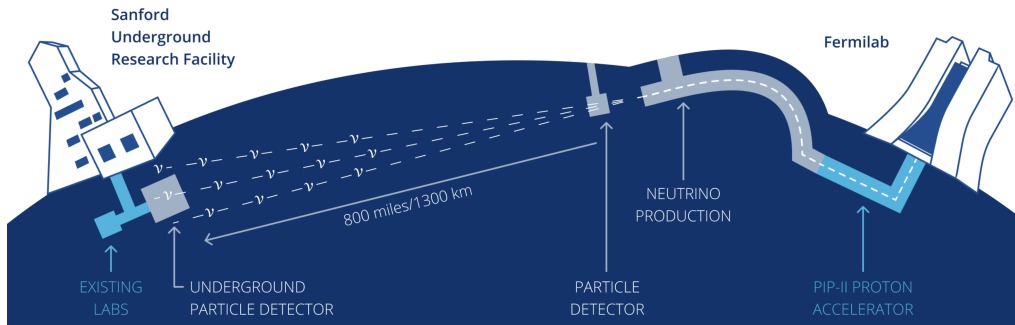
- 1 Background
- 2 Governing Equations
- 3 Numerical Methodology
- 4 Solver Parallelization
- 5 Test Cases
- 6 Summary and Future Work

Background

- Particle physics and Fermilab.
- Neutrino study (flavor transition, mass, CP symmetry violation, matter and antimatter, etc.).
- Particle detectors.
- The Deep Underground Neutrino Experiment ([DUNE](#)) project.
- [ProtoDUNE-SP](#) and ProtoDUNE-DP.
- Liquid argon time projection chamber ([LArTPC](#)).

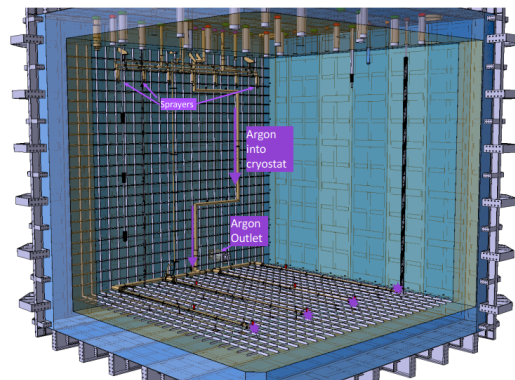
Background - DUNE

The Deep Underground Neutrino Experiment (DUNE) is an international flagship experiment to unlock the mysteries of neutrinos (<https://lbnf-dune.fnal.gov/>).



Background - ProtoDUNE

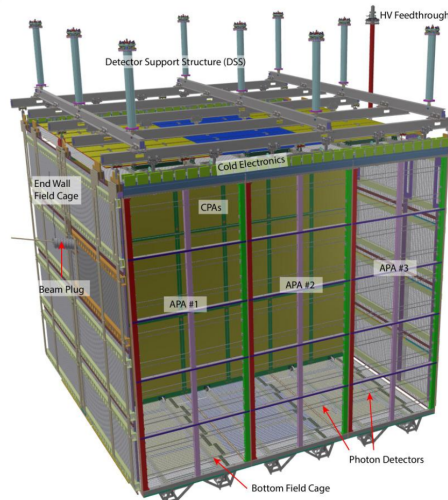
- Prototype of DUNE.
- still enormous about size of a 3-story house.
- 800 ton of liquid argon. (LArTPC)
- ProtoDUNE-SP and ProtoDUNE-DP.



ProtoDUNE-SP Cryostat

ProtoDUNE-SP - Field Cage

This image below helps to understand the components of the detector: **field cage walls**, **CPA plane**, **APA planes**.



What Happens inside LArTPC?

- In LArTPCs, the LAr flow field coexists with a strong electric field.
- High-speed charged particles like cosmic rays or neutrino beams ionize argon atoms producing electrons and positive ions.
- Electrons may attach to impurities (oxygen or water molecules) to produce negative ions.
- Electrons quickly swept away toward the anode by the electric field.
- Ions drift slowly at a speed comparable to the bulk flow speed.
- Therefore ions may accumulate locally in the flow field.
- Clustering of ions cause distortion of the electric field.
- The distorted electric field cause drifting electrons to arrive at different locations on the anode plane.

Outline

- 1 Background
- 2 Governing Equations
- 3 Numerical Methodology
- 4 Solver Parallelization
- 5 Test Cases
- 6 Summary and Future Work

Transport of Ions

The transport of ions can be modeled as

$$\frac{\partial \rho_c}{\partial t} + \nabla \cdot [(\mathbf{u} + \mathbf{u}_d)\rho_c] = \nabla \cdot (D\nabla \rho_c) + S \quad (1)$$

where

- ρ_c : the charge density of the positive ion.
- \mathbf{u} : the background flow velocity.
- \mathbf{u}_d : drifting velocity of the ions due to the electric field obtained via

$$\mathbf{u}_d = \mu \mathbf{E} \quad (2)$$

with μ being the mobility of the ions and \mathbf{E} the electric field.

- D : the diffusion coefficient, and
- S : the source/sink term

Electrostatic Potential

The electrostatic potential V satisfies the following Poisson equation according to Gauss's law

$$-\nabla \cdot (\nabla V) = \frac{\rho_c}{\varepsilon} \quad (3)$$

where ε is the permittivity of the medium which is defined as follows:

$$\varepsilon = \varepsilon_r \varepsilon_0. \quad (4)$$

with ε_r the relative permittivity (i.e. dielectric constant, $\varepsilon_r = 1.504$ for liquid argon) of the medium and $\varepsilon_0 = 8.854 \times 10^{-12}$ F/m the permittivity of free space (a vacuum).

The electric field \mathbf{E} is related to the electric potential V via

$$\mathbf{E} = -\nabla V \quad (5)$$

The interaction between the space charge and the electric field occurs as follows

- Electric field provides drifting velocity to the space charge transport equation.
- The space charge appears as the source term in the potential equation.

JACKSON
STATE
UNIVERSITY*

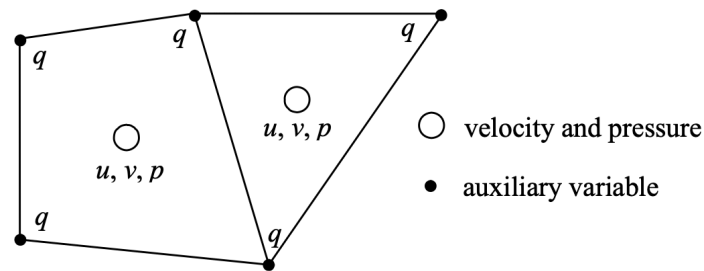
Outline

- 1 Background
- 2 Governing Equations
- 3 Numerical Methodology
- 4 Solver Parallelization
- 5 Test Cases
- 6 Summary and Future Work

Recall Hybrid FV/FE Method for Incompressible Flows

We have developed a hybrid FV/FE method for incompressible flows (Tu & Aliabadi, 2007)

- cell-centered FV method for the momentum equation.
- nodal FE method for the pressure Poisson equation.



Exact methodology can be applied to solve the current coupled transport-Poisson equations.

Overview of the Hybrid FV/FE Method

- The space charge transport equation (1) is a [linear advection-diffusion equation](#).
 - An implicit cell-centered finite volume method (FVM) is used to discretize this equation.
- The electric potential equation (3) is a [Poisson equation](#).
 - The nodal Galerkin finite element method (FEM) is chosen to discretize the Poisson equation.

Finite Volume Method for Ion Transport

The backward Euler difference formula (**BDF**) is adopted for the time integration. For each cell i , the finite volume discretization leads to

$$\frac{c_1 \rho_c^{n+1} + c_0 \rho_c^n + c_{-1} \rho_c^{n-1}}{\Delta t} + R(\rho_c^{n+1}) = 0 \quad \text{for each cell} \quad (6)$$

where ρ_c is the cell average of the unknown at cell i .

The system of Eq. (6) for all cells can be written in vector form as

$$\mathbf{G}(\boldsymbol{\rho}_c^{n+1}) = 0 \quad (7)$$

where the bold symbol $\boldsymbol{\rho}_c$ contains all unknowns at each of the cells.



Finite Volume Method for Ion Transport (cont)

- **Newton-Raphson** iterative method for the nonlinear equation system.
- Inside each nonlinear iteration, the Generalized Minimal RESidual method (**GMRES**) is used for solving the linear system.
- The Lower-Upper Symmetric Gauss Seidel (**LU-SGS**) preconditioning is used to improve the convergence of the GMRES solver.



Finite Element Method for Electric Potential

The unknown V_i is placed at each of the mesh vertices. With the help of nodal basis functions, one can express V at any location in the computational domain using the solutions at vertices

$$V = \sum_{j=1}^{nv} \phi_j V_j \quad (8)$$

where $\{\phi_j\}_{j=1}^{nv}$ are the nodal basis functions and nv is the number of vertices of the mesh.

The variational form of Eq. (3) is obtained by multiplying Eq. (3) with each of the shape functions and integrating over the entire domain Ω by parts as follows

$$\int_{\Omega} \nabla \phi_i \cdot \nabla V d\Omega = \int_{\Omega} \phi_i \frac{\rho_c}{\varepsilon} d\Omega + \int_{\Gamma} \phi_i (\mathbf{n} \cdot \nabla V) d\Gamma \quad i = 1, \dots, nv \quad (9)$$



Finite Element Method for Electric Potential (cont)

- Substituting Eq. (8) into Eq. (9) results in a **sparse and symmetric linear system**.
- The preconditioned **conjugate gradient method** is employed to solve this system.
- The preconditioning is based on the **Incomplete Lower-Upper (ILU(0))** decomposition.



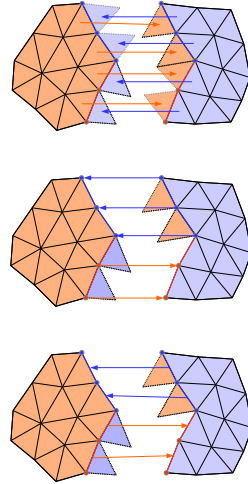
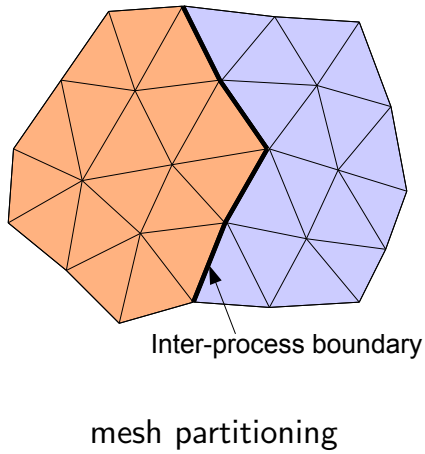
Outline

- 1 Background
- 2 Governing Equations
- 3 Numerical Methodology
- 4 Solver Parallelization
- 5 Test Cases
- 6 Summary and Future Work

Solver Parallelization

- Message Passing Interface ([MPI](#)).
- Single Program Multiple Data ([SPMD](#)) principle.
- ParMETIS for mesh partitioning.
- Very efficient non-blocking MPI functions can be called to set up the [inter-processor "gather" and "scatter" routines](#) in the pre-processing stage.

Inter-process Communication



Inter-process communication involves

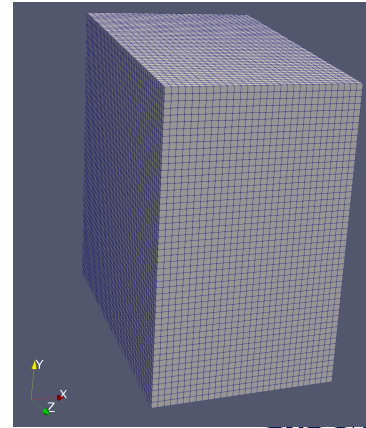
- cells (i.e. elements)
- vertices (i.e. nodes)
- faces

Outline

- 1 Background
- 2 Governing Equations
- 3 Numerical Methodology
- 4 Solver Parallelization
- 5 Test Cases
- 6 Summary and Future Work

Test case Setup

- The dimension data ($3.6\text{m} \times 6\text{m} \times 6\text{m}$) of the ProtoDUNE-SP detector volume is used to construct the computation domain $[0, 3.6] \times [-3, 3] \times [-3, 3]$.
- The anode plane is located at $x = 0\text{ m}$ and the cathode plane is at $x = 3.6\text{m}$. The remaining boundaries are the field cage walls.



Simulation Parameters

The following input parameters are given for the simulation:

- nominal electric field: $E_o = 500\text{V/cm}$,
- source term $S = 2 \times 10^{-10}\text{Cm}^{-3}\text{s}^{-1}$,
- dielectric constant $\epsilon_r = 1.504$ and permittivity of free space $\epsilon_0 = 8.854 \times 10^{-12}\text{F/m}$,
- mobility $\mu = 1.6 \times 10^{-7}\text{m}^2\text{V}^{-1}\text{s}^{-1}$, and
- diffusion coefficient $D = 1.2134543 \times 10^{-9}\text{m}^2/\text{s}$.

Note that some parameters are empirically determined and may cause uncertainties.

Simulation Setup

The time needed for ions to travel from the anode plane to the cathode plane
 $T = L_x / (\mu E_0) = 450\text{s}$.

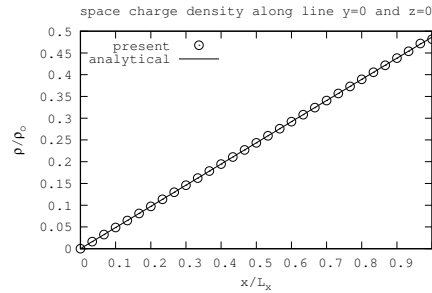
- In all simulations, the time step is chosen as $\Delta t = 7.5\text{s}$.
- Six CPU cores are used in parallel for this relatively small mesh.
- The simulation continues until the steady state has been reached.

Three Cases to Simulate

- **Case I:** Space Charge Transport under Uniform Electric Field.
- **Case II:** Interaction between the Space Charge Transport and the Electric Field without background flow field.
- **Case III:** Interaction between the Space Charge Transport and the Electric Field with the Effect of the Background Flow Field.

Case I: Space Charge Transport under Uniform Electric Field

- The electric field takes the uniform nominal value in x -direction across the chamber.
- Therefore, only the space charge transport equation is solved.
- BCs: Dirichlet condition $\rho_c = 0$ at the anode plane and open boundary condition at the cathode plane and at field cage walls.

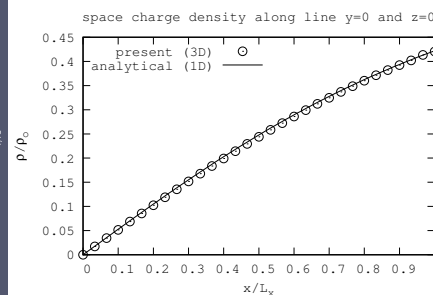
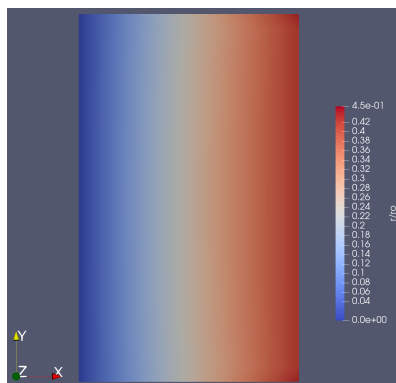


Case I: normalized space charge density distribution along the line defined by $y = 0$ and $z = 0$ in the case of uniform electric field.



Case II: Interaction between the Space Charge Transport and the Electric Field

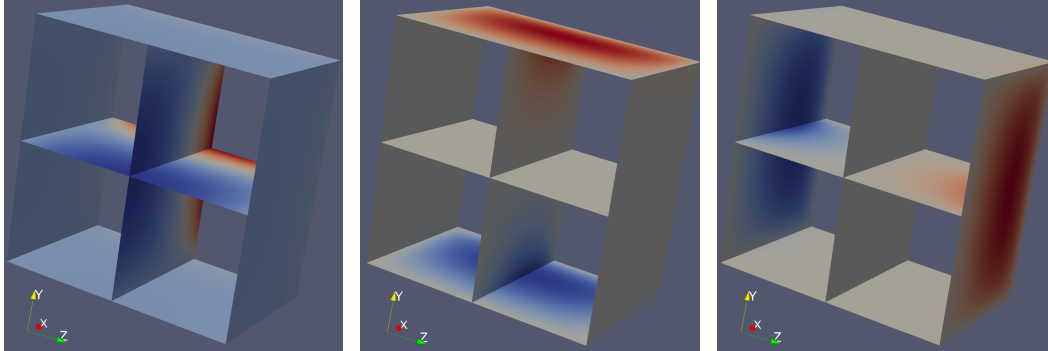
- This case couples the space charge transport equation and the electric potential Poisson equation in each time step.



Case II: space charge density distribution in the $x - y$ plane at $z = 0$ (left) and ρ_c/ρ_0 vs. x/L_x (right).



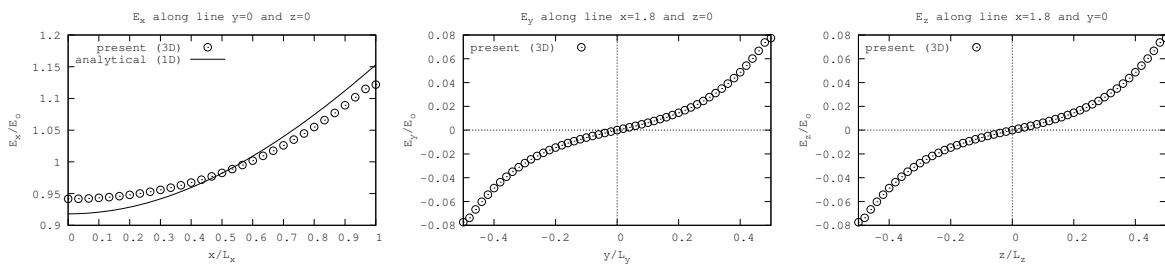
Case II: Distorted Electric Field



Case II: electric field maps in the center $x - y$ plane, the center $x - z$ plane and the field cage walls in the case of no background flow field. (left): x -component, (middle): y -component and (right): z -component.



Case II: Distorted Electric Field - Line Plots



Case II: electric field line plots. (left): E_x/E_0 vs. x/L_x along the line defined by $y = 0$ and $z = 0$, (middle): E_y/E_0 vs. y/L_y along the line defined by $x = 1.8$ and $z = 0$, and (right): E_z/E_0 vs. z/L_z along the line defined by $x = 1.8$ and $y = 0$. The electric field is normalized by the nominal electric field $E_0 = 500\text{V/cm}$.



Case III: The Effect of the Background Flow Field

- The drift velocity of ions is comparable in magnitude to the liquid argon flow field.
- The background flow field is expected to carry the ions around causing the local accumulation of space charges which further distorts the electric field.
- An artificial velocity field is confined in the $x - y$ plane with the following velocity components:

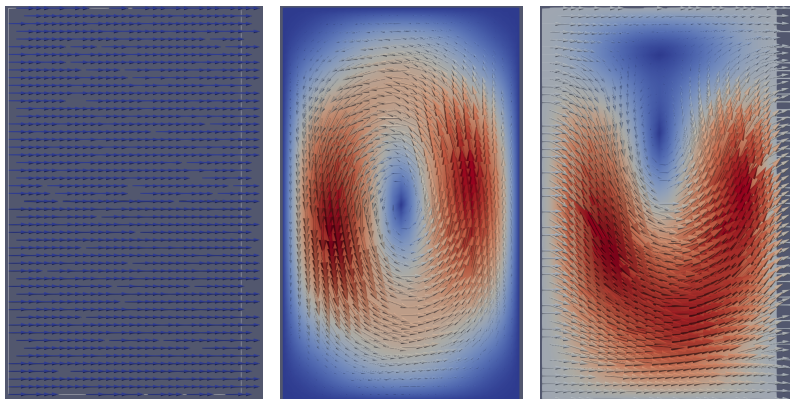
$$u_1 = \frac{1}{180}(x - x_l)^2(x_r - x)^2(y - y_b)(y_t - y)(y_b + y_t - 2y) \quad (10)$$

$$u_2 = -\frac{1}{180}(y - y_b)^2(y_t - y)^2(x - x_l)(x_r - x)(x_l + x_r - 2x) \quad (11)$$

$$u_3 = 0 \quad (12)$$

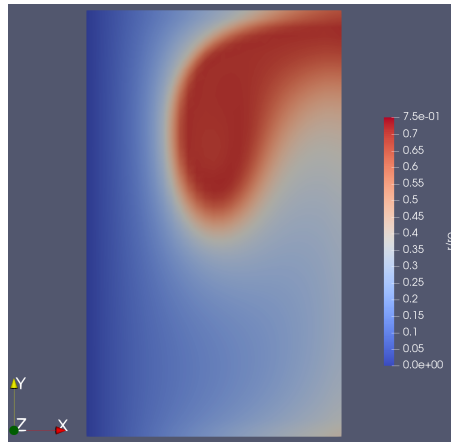
where $x_l = -3.6$, $x_r = 0.0$, $y_b = -3.0$ and $y_t = 3.0$ which define the $x - y$ dimensions of the detector chamber.

Case III: Velocity Field



Case III: velocity field in the center $x - y$ plane at the beginning of the simulation . (left): drift velocity field induced by the electric field, (middle): artificial flow field, and (right): combined velocity field.

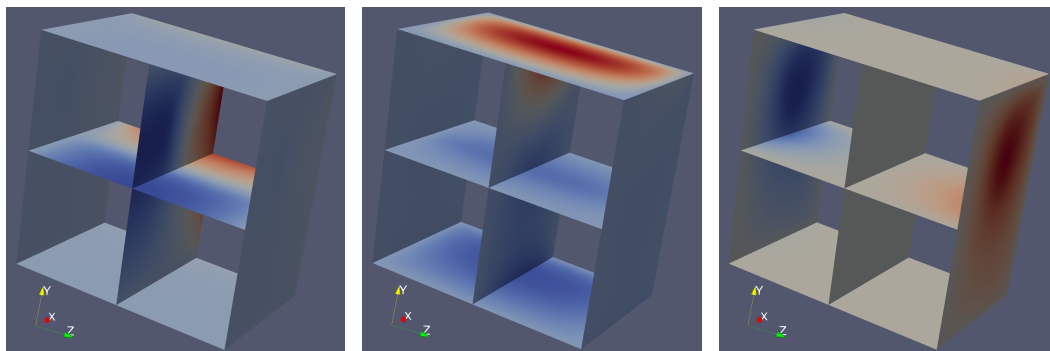
Case III: Space Charge Distribution



Case III: space charge density distribution in the $x - y$ plane at $z = 0$ in the presence of an artificial background flow velocity field.



Case III: Distorted Electric Field



Case III: electric field in the center $x - y$ plane, the center $x - z$ plane and the field cage walls in the presence of an artificial background flow field. (left): x -component, (middle): y -component, and (right): z -component.



Outline

- 1 Background
- 2 Governing Equations
- 3 Numerical Methodology
- 4 Solver Parallelization
- 5 Test Cases
- 6 Summary and Future Work

Summary

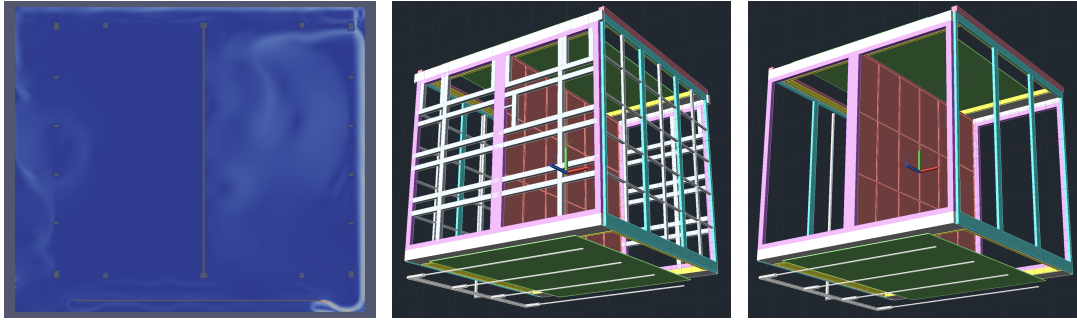
In this work, we have completed a hybrid finite volume/element solver to simulate the interaction between the positive ion transport and the electric field in a LArTPC detector.

- Implicit finite volume method for the ion transport.
- Continuous Galerkin finite element method for the electrostatic potential equation.
- The interaction between the space charge distribution and the electric field is numerically simulated within each physical time step.
- The comparison with the 1-D analytical solution verifies the accuracy of the current 3-D solver.
- Numerical tests show that the space charge effect on the electric field is noticeable and cannot be neglected.

The code has been transferred to our Fermilab collaborators. Users need to provide an externally generated flow velocity field as the input to the solver.

Ongoing Work

- Flow simulation of the 3D LArTPC detectors to obtain realistic flow field using our in-house incompressible flow solver. (ongoing)



Left: Velocity field of a 2D model. Middle and right: two versions of simplified geometry suitable for mesh generation.

Future Work

- Take into account of the effect of negative ions:
 - transport of impurities (H₂O and O₂) concentration.
 - electron attachment to impurities to generate negative ions.
- Compare to available experimental data and make parameter adjustments in the simulation to reduce the discrepancy.

Acknowledgments


This work is partially supported by

- U.S. Department of Energy Office of Science Award No. DE-SC0023125,
- NSF Award No. 2219542, and
- NASA Award No. 80NSSC21M0332.



THANK YOU

shuang.z.tu@jsums.edu

-  S. Tu, C. Jiang, T. Junk and T. Yang, "A Numerical Solver for Investigating the Space Charge Effect on the Electric Field in Liquid Argon Time Projection Chambers," *Journal of Instrumentation*, Vol. 18, 2023.
<https://iopscience.iop.org/article/10.1088/1748-0221/18/06/P06022>

